Hindawi Publishing Corporation
International Journal of Photoenergy
Volume 2006, Article ID 89638, Pages 1–9
DOI 10.1155/IJP/2006/89638

Temperature-Dependent Loop Formation Kinetics in Flexible Peptides Studied by Time-Resolved Fluorescence Spectroscopy

Harekrushna Sahoo, Andreas Hennig, and Werner M. Nau

School of Engineering and Science, International University Bremen, Campus Ring 1, 28759 Bremen, Germany

Received 20 February 2006; Accepted 16 April 2006

Looping rates in short polypeptides can be determined by intramolecular fluorescence quenching of a 2,3-diazabicyclo[2.2.2]oct-2-ene-labeled asparagine (Dbo) by tryptophan. By this methodology, the looping rates in glycine-serine peptides with the structure Trp-(Gly-Ser)$_n$-Dbo-NH$_2$ of different lengths ($n = 0$–10) were determined in dependence on temperature in D_2O and the activation parameters were derived. In general, the looping rate increases with decreasing peptide length, but the shortest peptide ($n = 0$) shows exceptional behavior because its looping rate is slower than that for the next longer ones ($n = 1, 2$). The activation energies increase from 17.5 kJmol^{-1} for the longest peptide ($n = 10$) to 20.5 kJmol^{-1} for the shortest one ($n = 0$), while the pre-exponential factors ($\log(A/\mathrm{s}^{-1})$) range from 10.20 to 11.38. The data are interpreted in terms of an interplay between internal friction (stiffness of the biopolymer backbone and steric hindrance effects) and solvent friction (viscosity-limited diffusion). For the longest peptides, the activation energies resemble more and more the value expected for solvent viscous flow. Internal friction is most important for the shortest peptides, causing a negative curvature and a smaller than ideal slope (ca. -1.1) of the double-logarithmic plots of the looping rates versus the number of peptide chain segments (N). Interestingly, the corresponding plot for the pre-exponential factors ($\log A$ versus $\log N$) shows the ideal slope (-1.5). While the looping rates can be used to assess the flexibility of peptides in a global way, it is suggested that the activation energies provide a measure of the "thermodynamic" flexibility of a peptide, while the pre-exponential factors reflect the "dynamic" flexibility.

1. INTRODUCTION

Since the paradigm of the lock-and-key principle [1] has been refined by the induced-fit model [2], molecular flexibility has emerged as a crucial factor determining the biological activity of proteins, for example, in substrate binding [3], antigenicity [4], or enzymatic activity [5]. The determination of flexible regions, however, is also essential for a detailed understanding of protein folding and for the characterization of the free energy landscape connecting the unfolded and native state of a protein [6]. In recent years, a number of studies [7–9] have attempted to determine the type of interactions/motions responsible for the rate-determining steps in protein folding. These studies have shown that the time scale of the elementary protein folding steps ranges from several nanoseconds to microseconds [10]. It has been recognized that the rate of intrachain (and in particular end-to-end) collision defines the important time-scale for the conversion of extended to collapsed conformations in the early stages of protein folding [11–13]. Knowledge of the local dynamics of the polypeptide backbone as imposed by the individual amino acid residues [14, 15] is therefore important.

Laser spectroscopy of short chromophore-labeled peptides has opened novel possibilities for investigating end-to-end collision kinetics in biopolymers, which is a critical parameter for loop or β-hairpin formation [16]. Looping rates are generally assessed by the probe/quencher methodology (Scheme 1). For this purpose, long-lived excited states are required as photophysical probes (P) along with diffusion-controlled contact quenchers (Q). The requirements are defined by the following limitations (see Scheme 1): (i) in the case of short-lived probes, diffusion to form the loop structure (k_+) is too slow to compete with the intrinsic excited-state decay (k_0) and does not cause sizable quenching effects. (ii) In the case of less efficient quenching, dissociation of the encounter complex between probe and quencher (k_-) competes, such that the intramolecular quenching rate constant (k_q) no longer corresponds to the looping rate (k_+).

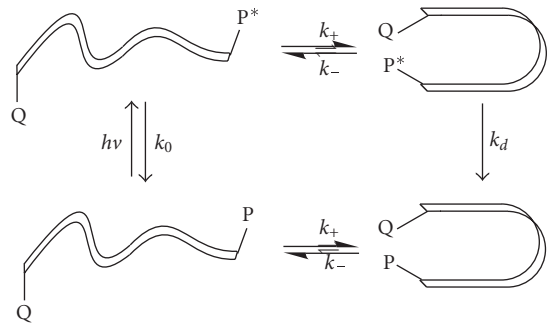

Scheme 1: Kinetic scheme for the determination of looping rates by the probe/quencher methodology.

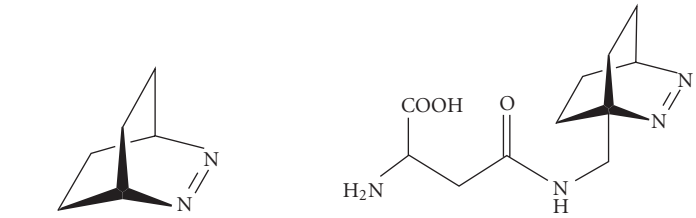

2, 3-diazabicyclo[2.2.2]oct-2-ene (DBO)

DBO-labeled asparagine (Dbo)

Scheme 2: Molecular structures of DBO and its asparagine derivative, Dbo.

(iii) In the case of distance-dependent quenching (as opposed to contact quenching) the elementary rate constants cannot be reliably determined.

Initial studies on end-to-end collision have employed transient absorption to monitor the quenching of triplet-excited states (either tryptophan (Trp) or aromatic ketones) by suitable quenchers [17–20]. Recently, we have introduced the quenching of 2,3-diazabicyclo[2.2.2]oct-2-ene (DBO, the chromophore with the longest fluorescence lifetime of organic molecules in solution, see Scheme 2) by Trp as an attractive fluorescence-based method to study loop formation kinetics in short polypeptides [21]. For this purpose, the chromophore was introduced through a labeled asparagine (Dbo, see Scheme 2) at one end of the peptide chain, and Trp was attached as a quencher to the other end. By this methodology, we have investigated the length dependence of loop formation in random-coiled polypeptides [21], the variation with the amino acid type (which has led to a flexibility scale for amino acids in peptides) [22], the dependence of peptide flexibility on the secondary structural motif [23], electrostatic effects [23], the effect of denaturants [24], β-peptides [24], polyprolines [24], and different quenchers like tyrosine [23].

Dbo is an attractive chromophore for biological studies due to its hydrophilicity, its small size, and its versatility in peptide synthesis. In fact, as an important practical application of our peptide flexibility studies, we have recently introduced a novel line of biological assays [25], which exploit the intramolecular quenching and concomitant lifetime shortening of Dbo in conformationally flexible Trp-labeled peptides (Scheme 3). Enzymatic cleavage removes this quenching pathway and results in the recovery of the exceedingly long fluorescence lifetime of Dbo (Scheme 3), which can be detected very accurately by employing the technique of nanosecond time-resolved fluorescence (Nano-TRF). Nano-TRF entails the application of a time-gate in the nanosecond range (see bottom decay trace in Scheme 3) to discriminate the fluorescence intensity of the long-lived probe (the "signal") from any other type of short-lived fluorescence due to uncleaved substrate, scattered excitation light, added compounds, enzyme cofactors, and so forth (the "background"). In this manner, relative to monitoring by steady-state fluorescence, an increase in signal-to-background ratio by several orders of magnitude can be readily achieved [25, 26].

As stated above, the principle of the protease assay in Scheme 3 rests on the flexibility of the uncleaved Dbo-Trp-labeled peptide, such that the development of additional Nano-TRF assays will be greatly assisted by a more accurate knowledge of the peptide flexibility, that is, the loop formation kinetics. In the present work, we have studied the temperature-dependence of intramolecular fluorescence quenching in short flexible Gly-Ser peptides in an effort to extract the activation energies for peptide loop formation or "peptide bending." Information on this temperature dependence is also directly relevant to Nano-TRF assays because (i) several enzymes require elevated temperatures for

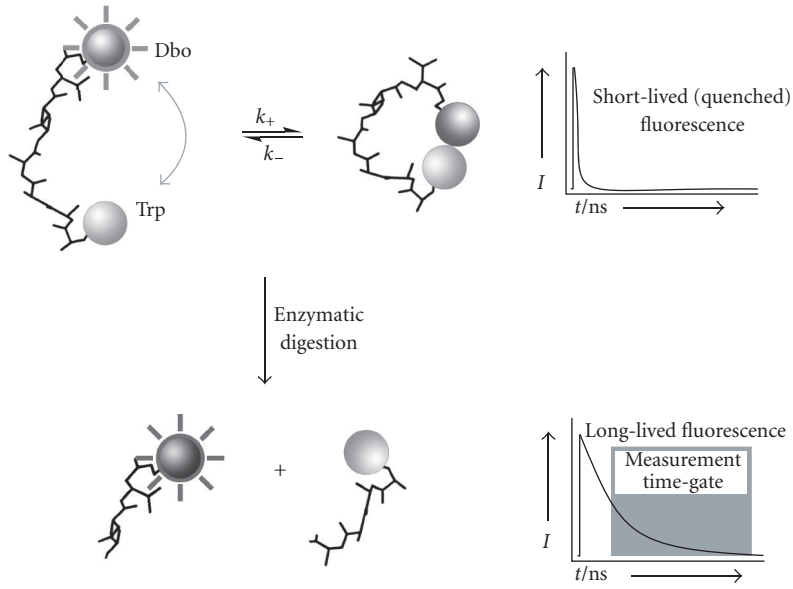

Scheme 3: Principle of protease assay based on probe/quencher-labeled substrates.

optimized activity, and (ii) the intramolecular quenching could potentially become more efficient at elevated temperatures and thereby further improve the lifetime differentiation of cleaved products from uncleaved substrate.

2. MATERIALS AND METHODS

Fmoc-protected Dbo was synthesized according to the literature procedure [21]. The probe/quencher-labeled peptides, Trp-(Gly-Ser)$_n$-Dbo-NH$_2$ (n = 0–10), as well as the corresponding reference peptides without quencher, (Gly-Ser)$_n$-Dbo-NH$_2$, were commercially synthesized in > 95% purity (Biosyntan, Berlin). Details on the synthesis of the probe and its suitability in solid-phase peptide synthesis are documented [21]. Water was nanopure quality (PURELAB) and D_2O was used as received from Applichem (99.8%D).

The fluorescence lifetimes of the water-soluble peptides were measured in D_2O under air at different temperatures by time-correlated single-photon counting (FLS920, Edinburgh Instruments Ltd.) using a PicoQuant diode laser LDH-P-C 375 (λ_{exc} = 373 nm, λ_{obs} = 450 nm, fwhm ca. 50 ps) for excitation. The temperature in the cuvette was controlled with a circulating water bath (Julabo F25/HD thermostat) through a feedback loop with a temperature-probe placed directly inside the cuvette to precisely maintain the target temperature within ± 0.1°C. Peptide concentrations were ca. 50 μM.

3. RESULTS

Intramolecular fluorescence quenching was investigated for glycine-serine peptides containing Dbo as fluorescent probe and Trp as quencher with the general structure Trp-(Gly-Ser)$_n$-Dbo (Scheme 4). The dependence on temperature (15-50°C) was investigated as well as the change with increasing chain length, that is, the peptides differed by the number of repetitive glycine-serine units with n = 0 to 10.

The fluorescence decays were recorded by time-correlated single photon counting in D_2O, in keeping with our previous studies [21–24]. The time-resolved fluorescence decays of all peptides were monoexponential, such that a specific fluorescence lifetime could be assigned to each peptide. It should be noted here that monoexponential fluorescence decays are not a priori expected in biopolymers as a consequence of conformational inhomogeneity, but were also previously observed and attributed to a fast equilibration of different conformations [21]. For some probe/quencher-labeled peptides (n = 2, 6, 10) a minor long-lived component with a pre-exponential factor of 1–4% was detected. For these samples, a biexponential fitting was performed, and the long-lived component was assigned to the quencher-unlabeled peptide as an impurity arising from imperfect solid-phase peptide synthesis (note that the peptide purity was very high, but only specified as > 95%).

To obtain accurate intramolecular quenching constants (k_q), the fluorescence lifetimes of the probe/quencher-labeled peptide (lifetime τ) as well as the corresponding probe-only-labeled peptide (τ_0) were determined and k_q was calculated according to (1) (see [21]). For the shortest and longest peptide (n = 0 and 10), the τ_0 values for the closest homologues (n = 1 and 6) were selected.

$$k_q = \frac{1}{\tau} - \frac{1}{\tau_0}. \quad (1)$$

Equation (1) explicitly "corrects" for the limited lifetime of the excited states, although the absolute corrections are quite small. This is because the lifetimes of the probe-only-labeled peptides are quite large (ca. 420–600 ns, at 25°C) compared to the probe/quencher-labeled ones (10–70 ns, at

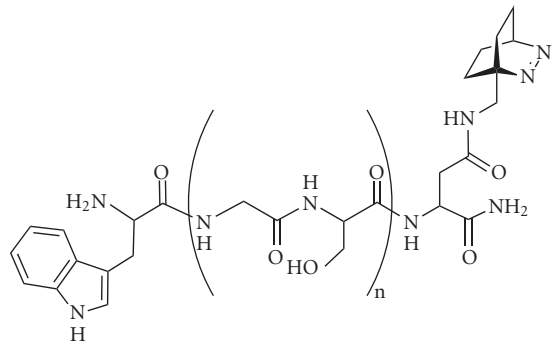

Scheme 4: Molecular structure of Trp-(Gly-Ser)$_n$-Dbo-NH$_2$ peptides.

Table 1: Dependence of the fluorescence lifetime on the length of Trp-(Gly-Ser)$_n$-Dbo-NH$_2$ probe/quencher-labeled peptides in D_2O at different temperatures.

n	τ/ ns[a]							
	15°C	20°C	25°C	30°C	35°C	40°C	45°C	50°C
0	31	25	22	19	17	15	14	12
1	17	15	13	11	10	9	8	7
2	24	21	17	16	14	12	11	10
3	31	27	24	21	19	17	15	14
4	36	32	28	23	22	19	18	16
6	51	45	39	34	30	28	25	23
10	87	76	69	60	54	49	45	42

[a]Error in lifetimes is ±3%.

25°C). All experimental τ and τ_0 values in dependence on peptide length and temperature are listed in Tables 1 and 2. Note that the lifetimes of the probe-only-labeled peptides (τ_0) showed a weaker temperature dependence than the lifetimes of the probe/quencher-labeled peptides (τ).

The resulting intramolecular fluorescence quenching rate constants are directly interpreted, following previously outlined arguments and control experiments [21, 23, 26], as rate constants for end-to-end collision or loop formation in the respective peptides ($k_q \approx k_+$). They are entered in Table 3.

For all peptides, the looping rates increased with increasing temperature, confirming an activation-controlled process (Table 3). The temperature-dependent rate constants afforded the activation parameters for loop formation according to the Arrhenius plots in Figure 1 [$\ln k_q(T) = \ln A - E_a/RT$]. As can be seen, the plots are strictly linear ($r^2 > 0.99$) in the investigated temperature range, such that the activation energies and pre-exponential factors could be obtained by linear regression analysis (Table 4); the activation energies cover a small range (17.5–20.5 kJmol^{-1}) but the variation is systematic: they gradually decrease upon increasing the peptide chain length.

As judged on the basis of the statistical error obtained from the regression analysis, the activation energies can be very accurately determined. However, we have reproduced the finding made in an earlier study [23] that although the looping rates in H_2O are generally 10–20% faster than in the slightly more viscous D_2O [27], this difference does not translate into significant differences of the activation energies (see values in square brackets in Table 4). This is interesting because the activation energy for solvent viscous flow in H_2O and D_2O differs by ca. 1 kJmol^{-1} [23] and should therefore become detectable, unless either other sources of error or different underlying reasons are involved.

In the initial study we have assumed a constant Dbo lifetime of 500 ns for probe-only-labeled glycine-serine peptides in D_2O [21]. The data in Table 2 show that this assumption is nicely justified, since the lifetimes fall within a 500 ± 100 ns range (25°C, Table 2). However, we noticed that they decrease systematically from 600 to 400 ns with increasing peptide length. An explicit correction for the lifetime of the probe-only-labeled peptides was therefore applied throughout this study to eliminate this source of systematic error. The correction terms in (1) ($1/\tau_0$) turned out to be very small, however, and did not significantly affect the intramolecular fluorescence quenching rate constants, and therefore the looping rates. In particular, all values determined in the present work at 20 and 25°C (which consider

Table 2: Dependence of the fluorescence lifetime on the length of (Gly-Ser)$_n$-Dbo-NH$_2$ probe-only-labeled peptides in D_2O at different temperatures.

n	τ_0/ ns[a]							
	15°C	20°C	25°C	30°C	35°C	40°C	45°C	50°C
1	666	623	587	549	529	510	491	477
2	585	533	486	465	438	418	393	373
3	557	508	469	441	418	395	374	351
4	530	483	452	418	397	372	354	330
6	488	450	420	384	370	347	323	304

[a]Error in lifetimes is ±5%.

Table 3: Dependence of looping rates on the length of Trp-(Gly-Ser)$_n$-Dbo-NH$_2$ peptides in D_2O at different temperatures.

n	$k_+/(10^7\ s^{-1})$[a]							
	15°C	20°C	25°C	30°C	35°C	40°C	45°C	50°C
0[b]	3.1	3.8	4.4	5.1	5.8	6.4	7.1	7.9
1	5.8	6.7	7.6	8.8	10.1	11.3	12.5	14.5
2	4.1	4.6	5.4	6.1	7.0	7.8	8.6	9.4
3	3.1	3.5	4.0	4.5	5.0	5.7	6.4	7.1
4	2.6	2.9	3.4	3.9	4.3	4.8	5.3	5.9
6	1.8	2.0	2.3	2.7	3.0	3.3	3.6	4.0
10[c]	0.9	1.1	1.2	1.4	1.6	1.8	1.9	2.1

[a]Determined by fluorescence quenching from (1) with the values from Tables 1 and 2; error is ± 5%. [b]Gly-Ser-Dbo-NH$_2$ was used as reference peptide for the τ_0 values. [c](Gly-Ser)$_6$-Dbo-NH$_2$ was used as reference peptide for the τ_0 values.

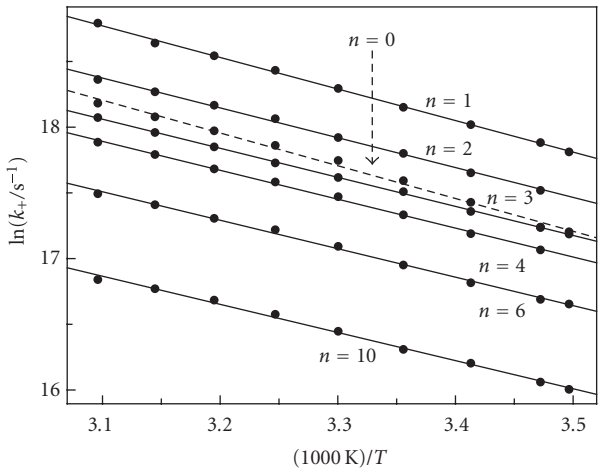

Figure 1: Arrhenius plots for the looping rates for Trp-(Gly-Ser)$_n$-Dbo-NH$_2$ peptides in D_2O; note that the dashed line refers to the shortest peptide ($n = 0$), which shows exceptional behavior (see text).

the actual τ_0 values in Table 2 for each peptide) bracket the values determined at 23°C in the previous study (which assumed a constant 500 ns value for τ_0) [21].

The decrease in intrinsic lifetime of the Dbo chromophore (τ_0) with increasing peptide length could be due to two reasons. First, as the peptides become longer, the microenvironment of the Dbo chromophore changes to a more "organic" one. This results, in particular, in an enhanced local polarizability/refractive index, which is known to increase the radiative decay rate and thereby shorten the fluorescence lifetime of Dbo [28]. Second, although glycine and serine showed negligible quenching effects in intermolecular experiments in D_2O [21], a slight intramolecular quenching especially by serine appeared viable, since the DBO fluorescence is known to be quenched in alcoholic solvents [29, 30].

The quenching mechanism by alcohols was identified, on the basis of very large deuterium solvent isotope effects (up to 20), as an aborted hydrogen atom abstraction from the O−H bonds (note that the O−H bond in alcohols is much weaker than that of water, which itself is a much weaker quencher) [29]. In fact, when the lifetimes of different peptides were compared in H_2O and D_2O (Table 5), a slightly larger quenching effect was observed in H_2O, but the data are too limited to unambiguously identify the quenching by the serine O−H bonds as the dominant factor modulating the lifetimes of Dbo. To summarize, the lifetime variation presents an interesting mechanistic peculiarity, which has no significant effect on the interpretation of the looping rates. This applies especially when the measurements are performed in D_2O [21], where Dbo has a longer lifetime, which further reduces the correction term in (1).

4. DISCUSSION

In the present study, we have investigated the temperaturedependence of the looping rates for glycine-serine polypeptides of different lengths. As spectroscopic handle, we employed

Table 4: Dependence of the activation energies and pre-exponential factors for loop formation on the length of Trp-(Gly-Ser)$_n$-Dbo-NH$_2$ peptides in D_2O.

n	E_a/(kJ/mol)	$\log(A/s^{-1})$
0	20.5 ± 0.6	11.23 ± 0.10
1	19.9 ± 0.2	11.38 ± 0.05
2	18.9 ± 0.3	11.03 ± 0.05
3	18.4 ± 0.1	10.81 ± 0.05
4	18.3 ± 0.3	10.73 ± 0.05
6	18.0 ± 0.4[17.9 ± 0.1][a]	10.51 ± 0.05[10.55 ± 0.05][a]
10	17.8 ± 0.4	10.20 ± 0.10

[a]Value measured in H_2O.

Table 5: Dependence of the intrinsic fluorescence lifetime of Dbo (in the absence of Trp as quencher) on peptide length in (Gly-Ser)$_n$-Dbo-NH$_2$ peptides at 25°C.

n	$\tau(H_2O)$/ns	$\tau(D_2O)/ns$	origin of peptide
0	360	573	protease cleavage [a]
1	329	587	synthetic
2	263 [251][a,b]	486	synthetic
4	237	452	synthetic
6	224	420	synthetic
7	227	—	protease cleavage [a]

[a]Peptide was obtained by protease cleavage from a suitable precursor peptide in phosphate buffer (pH 7, H_2O), unpublished results. [b]Data in brackets refer to (Gly-Ser)$_2$-Dbo-Gly-Ser-OH.

the intramolecular quenching of the long-lived fluorescent state of Dbo (attached to one end of the peptide) by Trp (attached to the other end). Formal kinetic treatment for the excited-state reaction pathways in Scheme 1 predicts that the experimental fluorescence quenching rate constant (k_q) is related to the association (k_+), dissociation (k_-), and deactivation (k_d) rate constants for the encounter complex by (2):

$$k_q = \frac{k_+ k_d}{k_- + k_d}. \quad (2)$$

Owing to the efficient quenching in the Dbo-Trp probe/quencher pair, $k_d \gg k_-$ holds, such that (2) becomes $k_q \approx k_+$ [24], that is, the experimental fluorescence quenching rate constant (obtained according to (1) from the fluorescence lifetimes) provides a direct measure of the looping rate constant.

The reasons for the choice of the glycine-serine peptides were threefold: first, glycine-serine peptides are presumed to be "structureless" and to adopt a random coil conformation, such that equilibria with stable secondary structures did not need to be considered [17, 21]. Second, they are known to be highly flexible as shown by previous measurements at ambient temperature [17, 21], and third, both glycine and serine have a high abundance in turn and loop sequences [31], and may therefore play a key role in the early stages of protein folding. It should be noted that the presently determined looping rates are in excellent agreement with the previous data [21], that is, the values at 20°C are equal to or slightly lower than the previous rate constants at 23°C, while the presently reported values at 25°C are slightly larger. This is satisfying because the present data were obtained in a different laboratory with a different experimental setup and a more advanced excitation source (diode laser versus flash lamp) and confirm the reproducibility of the results obtained by the fluorescence quenching method.

At all temperatures, the double-logarithmic plots of the looping rate constants against the number of peptide bonds (taken as the number of amide bonds, i.e., including the additional amide linkage in the Dbo side chain) reveal the characteristic negative curvature and the inversion for the shortest dipeptide at all temperatures (Figure 2) (see [21]).

We have recently provided the first activation energies for loop formation of short peptides [23] (as well as oligonucleotides [32]) corresponding to the strand and turn regions of the protein ubiquitin. Subsequently, additional values have been obtained by the triplet quenching technique [18], but the two techniques (time-correlated single photon counting versus photomultiplier-based transient absorption) differ too much in terms of data accuracy to allow further comparison. Our present work provides the first systematic report on the variation of the activation energies for loop formation with peptide length. The experimental data are shown in Table 4 and Figure 1.

The looping rates increase with increasing temperature, and this increase (from 15–50°C) is more pronounced for the shortest peptide (factor 2.6, $n = 0$) than for the longest one (factor 2.2, $n = 10$). This translates into a systematic decrease of the activation energy for loop formation as the backbone becomes longer, that is, from 20.5 kJmol^{-1} for $n = 0$ to 17.8 kJmol^{-1} for $n = 10$. The absolute numbers are of

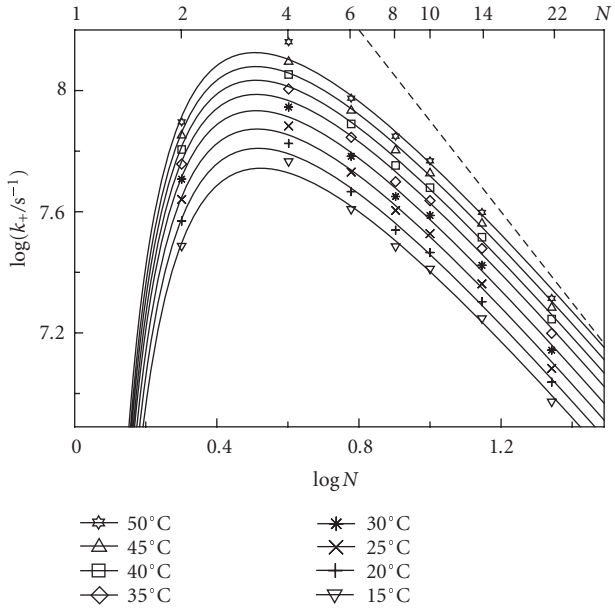

Figure 2: Double logarithmic plot of the looping rates (k_+) at different temperatures versus the peptide length, taken as the number of intervening amide bonds (N). A simple function of the type $y = a - 1.5x - b/x$ was fitted to the experimental data to reflect the theoretical slope of -1.5 at long chain lengths and the expected falloff (b/x) term at short chain lengths. The dashed line has a slope of -1.5 and is shown to illustrate the deviation from theoretical behavior.

interest in relation to the activation energy for solvent viscous flow (16.6 kJmol^{-1} for D_2O [23]). As the chain length increases, loop formation becomes more and more controlled by solvent friction and the activation energy therefore approaches the activation energy for solvent viscous flow. For the shorter peptides, the stiffness of the peptide backbone comes into play, which adds to the activation barrier (internal friction). This raises the activation barrier significantly by ca. 3–4 kJmol^{-1}. The higher activation energy of the shorter peptides should translate into lower diffusion coefficients of the chain ends, which have been theoretically implicated [33], but not yet experimentally corroborated.

The significant internal friction is also held responsible for the negative curvature of the double-logarithmic plot in Figure 2 at short chain lengths. The two experimental findings, namely the slower-than-expected looping rates in short peptides along with significant internal friction in these cases, jointly reflect significant deviations from ideal-chain behavior, which are also expected from several theoretical studies [33–36]. Glycine-serine biopolymers do therefore behave more ideally at longer chain length, and the slope of the double-logarithmic plots does indeed asymptotically approach the ideal-chain value (derived from first principles polymer theory [37, 38]) of -1.5 in long chains. Note that the dashed line in Figure 2 reflects this theoretical slope and that the fitted lines in Figure 2 refer to a trial function with exactly this slope, that is, $y = a - 1.5x - b/x$.

The absolute activation energies for the glycine-serine peptides are small, however, which is due to the fact that the amino acids glycine and serine are the most "flexible" ones on the amino acid flexibility scale [22]. For peptides lacking these flexible segments, larger activation energies have been observed (up to 25 kJ/mol) [23]. In these cases the contribution of internal friction is more significant because the peptides contain no flexible amino acids. However, the introduction of a single glycine appears to be sufficient to bring the values, within error, into the presently observed range [23].

In the previous study, we have compared three equally long peptides and found a correlation between the absolute looping rates and the activation energies [23]. For the present glycine-serine series, such a correlation does not hold, because the peptide length is being varied; in fact, the glycine-serine peptides with the highest looping rates (Table 3) do not show the smallest activation barriers, but instead the largest ones (Table 4).

The pre-exponential factors provide also interesting information. If the data in the double-logarithmic plots in Figure 2 (but ignoring the shortest dipeptide with $n = 0$, which is an exceptional case) are fitted by a simple linear regression line, slopes between -1.06 (15°C) to -1.10 (50°C) are obtained, which fall far below the theoretical value for the ideal-chain behavior (-1.5). This is expected due to the interference of differential internal friction (see above). However, since the differential friction manifests itself in the activation energies, the pre-exponential factors ($\log A$ in Table 4) should be devoid of this complication. Specifically, they should reflect the looping rates in the absence of any activation barrier and therefore provide a much better manifestation of ideal chain behavior. Much to our surprise, the correlation of the $\log A$ versus the $\log N$ values was indeed found to be linear (Figure 3). Moreover, the slope was larger than that for the direct correlations of the looping rates (Figure 2) and, in addition, the slope (-1.53 ± 0.07) matched, within error, that expected for the ideal chain.

It transpires from the present results that loop formation can be characterized by three characteristic parameters: the rate constant, the activation energy, and the pre-exponential factor. We have previously interpreted the looping rate constants in terms of a "global" flexibility of the peptide backbone [22]. Inspection of the activation parameters allows one to refine this concept by assigning a "thermodynamic" flexibility in terms of the activation energies and an intrinsic "dynamic" flexibility in terms of the pre-exponential factors. The latter provides a measure of how "floppy" the peptide would be if the chain would be allowed to move in a barrierless way. The former reports on relative peptide stiffness, the ease of peptide bending, and the barriers for conformational motions as well as steric hindrance effects. Accordingly, there are different ways to characterize the flexibility or stiffness of a peptide backbone. A comparison of looping rates is therefore difficult and is only meaningful if either the dynamic or the thermodynamic flexibility is approximately kept constant, for example, by comparing peptides with the same

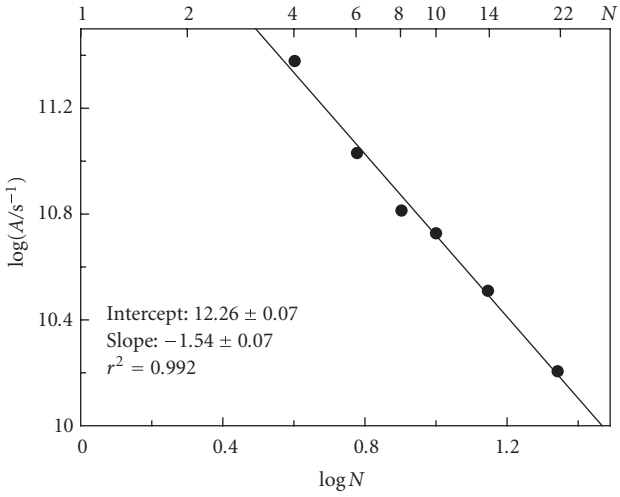

Figure 3: Double logarithmic plot of the pre-exponential factors for loop formation (Table 4) versus the peptide length, taken as the number of intervening amide bonds (N).

length but different structures [22, 23], or by comparing peptides of similar structure but different lengths [21, this work]. Finally, it is important to note that the activation parameters should not be overinterpreted, since it is unknown to which extent enthalpy-entropy correlation effects apply in the loop formation process. The large pre-exponential factors previously observed for the peptides with the slowest looping rates [23], and the decreased pre-exponential factor for the shortest dipeptide ($n = 0$) in the present series show that exceptional cases exist.

5. CONCLUSIONS

The determination of the temperature dependence of the looping rates affords interesting insights into the "dynamic" versus "thermodynamic" flexibility of polypeptides and the interplay between internal and solvent friction. Loop formation in short glycine-serine polypeptides is slowed by internal friction, which results in increased activation barriers. In contrast, the pre-exponential factors for loop formation follow ideal-chain behavior with the exception of the shortest (di)peptide. These experimental results are in agreement with theoretical predictions [33–36] and reveal more of the potential of the Dbo-based fluorescence quenching technique for determining loop formation kinetics. The Dbo/Trp probe/quencher technique excels not only with respect to convenient measurement (in water under air), high sensitivity (10–100 μM range), and highest precision as well as reproducibility (Poissonian error statistics in time-correlated single photon counting), but also with respect to the transferability of the fundamental kinetic measurements to practical applications, namely Nano-TRF fluorescence protease assays suitable for high-throughput screening in drug discovery [25].

ACKNOWLEDGMENT

This work was carried out within the graduate program "Nanomolecular Science" at the International University Bremen.

REFERENCES

[1] E. Fischer, "Einfluss der Configuration auf die Wirkung der Enzyme," *Berichte der Deutschen Chemischen Gesellschaft*, vol. 27, pp. 2985–2993, 1894.

[2] D. E. Koshland Jr., "Application of a theory of enzyme specificity to protein synthesis," *Proceedings of the National Academy of Sciences of the United States of America*, vol. 44, no. 2, pp. 98–104, 1958.

[3] D. T. Braddock, J. M. Louis, J. L. Baber, D. Levens, and G. M. Clore, "Structure and dynamics of KH domains from FBP bound to single-stranded DNA," *Nature*, vol. 415, no. 6875, pp. 1051–1056, 2002.

[4] N. Taschner, S. A. Müller, V. R. Alumella, et al., "Modulation of antigenicity related to changes in antibody flexibility upon lyophilization," *Journal of Molecular Biology*, vol. 310, no. 1, pp. 169–179, 2001.

[5] P. Závodszky, J. Kardos, A. Svingor, and G. A. Petsko, "Adjustment of conformational flexibility is a key event in the thermal adaptation of proteins," *Proceedings of the National Academy of Sciences of the United States of America*, vol. 95, no. 13, pp. 7406–7411, 1998.

[6] H. J. Dyson and P. E. Wright, "Intrinsically unstructured proteins and their functions," *Nature Reviews Molecular Cell Biology*, vol. 6, no. 3, pp. 197–208, 2005.

[7] K. W. Plaxco and D. Baker, "Limited internal friction in the rate-limiting step of a two-state protein folding reaction," *Proceedings of the National Academy of Sciences of the United States of America*, vol. 95, no. 23, pp. 13591–13596, 1998.

[8] M. Jacob, T. Schindler, J. Balbach, and F. X. Schmid, "Diffusion control in an elementary protein folding reaction," *Proceedings of the National Academy of Sciences of the United States of America*, vol. 94, no. 11, pp. 5622–5627, 1997.

[9] O. Bilsel and C. R. Matthews, "Barriers in protein folding reactions," *Advances in Protein Chemistry*, vol. 53, pp. 153–207, 2000.

[10] S. A. Pabit, H. Roder, and S. J. Hagen, "Internal friction controls the speed of protein folding from a compact configuration," *Biochemistry*, vol. 43, no. 39, pp. 12532–12538, 2004.

[11] S. E. Jackson and A. R. Fersht, "Folding of chymotrypsin inhibitor 2. 1. evidence for a two-state transition," *Biochemistry*, vol. 30, no. 43, pp. 10428–10435, 1991.

[12] A. Ansari, C. M. Jones, E. R. Henry, J. Hofrichter, and W. A. Eaton, "The role of solvent viscosity in the dynamics of protein conformational changes," *Science*, vol. 256, no. 5065, pp. 1796–1798, 1992.

[13] S. J. Hagen, C. W. Carswell, and E. M. Sjolander, "Rate of intrachain contact formation in an unfolded protein: temperature and denaturant effects," *Journal of Molecular Biology*, vol. 305, no. 5, pp. 1161–1171, 2001.

[14] C. M. Dobson, "Unfolded proteins, compact states and molten globules," *Current Opinion in Structural Biology*, vol. 2, no. 1, pp. 6–12, 1992.

[15] D. J. Segel, A. Bachmann, J. Hofrichter, K. O. Hodgson, S. Doniach, and T. Kiefhaber, "Characterization of transient intermediates in lysozyme folding with time-resolved small-angle X-ray scattering," *Journal of Molecular Biology*, vol. 288, no. 3, pp. 489–499, 1999.

[16] J. Kubelka, J. Hofrichter, and W. A. Eaton, "The protein folding 'speed limit '," *Current Opinion in Structural Biology*, vol. 14, no. 1, pp. 76–88, 2004.

[17] O. Bieri, J. Wirz, B. Hellrung, M. Schutkowski, M. Drewello, and T. Kiefhaber, "The speed limit for protein folding measured by triplet-triplet energy transfer," *Proceedings of the National Academy of Sciences of the United States of America*, vol. 96, no. 17, pp. 9597–9601, 1999.

[18] F. Krieger, A. Möglich, and T. Kiefhaber, "Effect of proline and glycine residues on dynamics and barriers of loop formation in polypeptide chains," *Journal of the American Chemical Society*, vol. 127, no. 10, pp. 3346–3352, 2005.

[19] L. J. Lapidus, W. A. Eaton, and J. Hofrichter, "Measuring the rate of intramolecular contact formation in polypeptides," *Proceedings of the National Academy of Sciences of the United States of America*, vol. 97, no. 13, pp. 7220–7225, 2000.

[20] L. J. Lapidus, W. A. Eaton, and J. Hofrichter, "Dynamics of intramolecular contact formation in polypeptides: distance dependence of quenching rates in a room-temperature glass," *Physical Review Letters*, vol. 87, no. 25, pp. 258101/1–258101/4, 2001.

[21] R. R. Hudgins, F. Huang, G. Gramlich, and W. M. Nau, "A fluorescence-based method for direct measurement of submicrosecond intramolecular contact formation in biopolymers: an exploratory study with polypeptides," *Journal of the American Chemical Society*, vol. 124, no. 4, pp. 556–564, 2002.

[22] F. Huang and W. M. Nau, "A conformational flexibility scale for amino acids in peptides," *Angewandte Chemie International Edition*, vol. 42, no. 20, pp. 2269–2272, 2003.

[23] F. Huang, R. R. Hudgins, and W. M. Nau, "Primary and secondary structure dependence of peptide flexibility assessed by fluorescence-based measurement of end-to-end collision rates," *Journal of the American Chemical Society*, vol. 126, no. 50, pp. 16665–16675, 2004.

[24] F. Huang and W. M. Nau, "Photochemical techniques for studying the flexibility of polypeptides," *Research on Chemical Intermediates*, vol. 31, no. 7-8, pp. 717–726, 2005.

[25] A. Hennig, D. Roth, T. Enderle, and W. M. Nau, "Nanosecond time-resolved fluorescence protease assays," *ChemBioChem*, vol. 7, no. 5, pp. 733–737, 2006.

[26] W. M. Nau, F. Huang, X. Wang, H. Bakirci, G. Gramlich, and C. Marquez, "Exploiting long-lived molecular fluorescence," *Chimia*, vol. 57, no. 4, pp. 161–167, 2003.

[27] C. H. Cho, J. Urquidi, S. Singh, and G. W. Robinson, "Thermal offset viscosities of liquid H_2O , D_2O, and T_2O," *Journal of Physical Chemistry B*, vol. 103, no. 11, pp. 1991–1994, 1999.

[28] J. Mohanty and W. M. Nau, "Refractive index effects on the oscillator strength and radiative decay rate of 2,3-diazabicyclo[2.2.2]oct-2-ene," *Photochemical and Photobiological Sciences*, vol. 3, no. 11-12, pp. 1026–1031, 2004.

[29] W. M. Nau, G. Greiner, H. Rau, M. Olivucci, and M. A. Robb, "Discrimination between hydrogen atom and proton abstraction in the quenching of n, π^* singlet-excited states by protic solvents," *Berichte der Bunsen-Gesellschaft für Physikalische Chemie*, vol. 102, no. 3, pp. 486–492, 1998.

[30] W. M. Nau, G. Greiner, H. Rau, J. Wall, M. Olivucci, and C. Scaiano, "Fluorescence of 2,3-diazabicyclo[2.2.2]oct-2-ene revisited: solvent-induced quenching of the n, π^*-excited state by an aborted hydrogen atom transfer," *Journal of Physical Chemistry A*, vol. 103, no. 11, pp. 1579–1584, 1999.

[31] J. M. Berg, J. L. Tymoczko, and L. Stryer, *Biochemistry*, W. H. Freeman, New York, NY, USA, 2003.

[32] X. J. Wang and W. M. Nau, "Kinetics of end-to-end collision in short single-stranded nucleic acids," *Journal of the American Chemical Society*, vol. 126, no. 3, pp. 808–813, 2004.

[33] X. Wang, E. N. Bodunov, and W. M. Nau, "Fluorescence quenching kinetics in short polymer chains: dependence on chain length," *Optics and Spectroscopy*, vol. 95, no. 4, pp. 560–570, 2003.

[34] C. J. Camacho and D. Thirumalai, "Theoretical predictions of folding pathways by using the proximity rule, with applications to bovine pancreatic trypsin inhibitor," *Proceedings of the National Academy of Sciences of the United States of America*, vol. 92, no. 5, pp. 1277–1281, 1995.

[35] I.-C. Yeh and G. Hummer, "Peptide loop-closure kinetics from microsecond molecular dynamics simulations in explicit solvent," *Journal of the American Chemical Society*, vol. 124, no. 23, pp. 6563–6568, 2002.

[36] C. Hyeon and D. Thirumalai, "Kinetics of interior loop formation in semiflexible chains," *Journal of Chemical Physics*, vol. 124, no. 10, pp. 14 pages, 2006.

[37] U. W. Suter, M. Mutter, and P. J. Flory, "Macrocyclization equilibria .2. poly(dimethylsiloxane)," *Journal of the American Chemical Society*, vol. 98, no. 19, pp. 5740–5745, 1976.

[38] M. Mutter, U. W. Suter, and P. J. Flory, "Macrocyclization equilibria .3. poly(6-aminocaproamide)," *Journal of the American Chemical Society*, vol. 98, no. 19, pp. 5745–5748, 1976.